

United Nations Educational, Scientific and Cultural Organization  
and  
International Atomic Energy Agency

THE ABDUS SALAM INTERNATIONAL CENTRE FOR THEORETICAL PHYSICS

**AN EMPIRICAL FORMULA FOR INNER-SHELL IONIZATION OF ATOMS**

A.K.F. Haque<sup>1</sup>

*Department of Physics, University of Rajshahi, Rajshahi 6205, Bangladesh  
and*

*The Abdus Salam International Centre for Theoretical Physics, Trieste, Italy,*

M.R. Talukder

*Department of Applied Physics and Electronic Engineering, University of Rajshahi,  
Rajshahi 6205, Bangladesh,*

M. Shahjahan, M.A. Uddin and A.K. Basak

*Department of Physics, University of Rajshahi, Rajshahi 6205, Bangladesh.*

**Abstract**

Electron impact single ionization cross sections (EIICS) of 40 *K*-, 11 *L*-, 3 *M*-shell and 3 *L*-subshell atomic targets, ranging from H to U, are evaluated using the generalized parameters of recently propounded analytical model [Campos C. S, *et al* 2007, J. Phys. B: At. Mol. Opt. Phys. 40, 3835] by incorporating the relativistic and ionic factors in it. Six sets of parameters, each for the *K*-, *L*-, *M*-shell and *L*<sub>1</sub>-, *L*<sub>2</sub>-, and *L*<sub>3</sub>-subshell provide an excellent account of the experimental EIICS data of atomic targets for the incident energies from threshold up to 2 GeV for *K*-shell and up to about 900 MeV for *L*-shell, *L*-subshell and *M*-shell, respectively. In comparison with the quantum mechanical and analytical predictions, it is found that the calculated cross sections using the present model are in better agreement with the experimental results.

MIRAMARE – TRIESTE

July 2009

---

<sup>1</sup> Regular Associate of ICTP. [ahaque@ictp.it](mailto:ahaque@ictp.it), [fhaque2001@yahoo.com](mailto:fhaque2001@yahoo.com)

## 1. Introduction

The last few decades have produced both theoretical and experimental data for cross sections of inner-shell ionization. The knowledge of these cross sections has not only fundamental importance for the understanding collision dynamics of electron-atom interactions, etc. but is also used extensively in many applied fields such as radiation science, astrophysics, plasma physics and elemental analysis using electron probe microanalysis (EPMA), Auger electron spectroscopy (AES), electron energy loss spectroscopy (EELS), transmission electron microscopy (TEM). Quantum mechanical calculations and experiments generate cross sections at some specific energies and target atoms suitable for calculations or experiments. The ab initio calculations usually based on various approximations, are lengthy and hence time-consuming. Despite these cumbersome efforts, the results are not always satisfactory, as one should expect. The applied areas, as mentioned earlier, need enormous and continuous data for cross sections for targets over wide ranges of incident energies with desired accuracy. This can be met best through the use of an analytical formula producing rapid generation of cross sections with reasonable accuracy and a wide range of applicability as regards species of targets and incident energies.

Analytical models with species dependent parameters are available in the literature. However, these models cannot be used for the absolute values of cross sections wherever theoretical calculations and experimental data are not available to fit the data for obtaining the optimal values of the parameters of the models and then applied to any desired incident energy. This fact underscores the need for the generalization of the parameters of an analytical model as far as possible while keeping the accuracy to the desired level.

Excellent reviews concerning theoretical calculations and experimental measurements have been provided by Powell [1,2]. In a pioneering work, Bethe [3,4] developed a formula to compute inner-shell ionization (ISI) cross sections, based on plane wave Born approximation (PWBA) valid for high energies. Semiempirical modifications of PWBA have been proposed [5,6] to describe data also at low energies. Other analytical models include classical and semi-classical formulations by [7,8,9]. Finally, a large number of empirical and semiempirical models have been proposed to describe the electron impact  $K$ -shell ionization cross section as a function of the incident energies [10,11,12]. However, each of these formulae have limited domain of applicability and no effort has been made for the calculation of ISI of the  $L$ - and  $M$ -shell ionization cross-sections of atoms.

Campos et al [13] proposed an analytical model to describe the  $K$ - and  $L$ -shell ionization of atoms over a wide range of atomic numbers  $4 < Z < 79$ . The formula has been based on the calculations of ionization cross section values obtained using distorted wave Born approximation

(DWBA). But the model is applicable for overvoltages  $U \leq 10$  (where  $U = E/I$ ,  $E$  is the incident energy and  $I$  is the ionization potential). The formula has not been applied to the calculations of  $M$ -shell ionization cross sections.

The purpose of this work is to extend the energy domain of applicability of the model by incorporating into it the Gryzniski type relativistic factor [7] and ionic factor to improve its accuracy of calculation. The values of the parameters of the models are determined in order to get the best fit to the available  $K$ -,  $L$ -,  $M$ -shell, and  $L$ -subshell ionization cross section data. The model so framed is referred to as SAKLM model.

## 2. Outline of the model

Campos et al proposed an analytical model to describe the absolute cross sections of  $K$ - and  $L$ -shell ionization cross section of atoms. This model reads

$$\sigma_{old}(U) = \frac{A_n(Z)}{B_n(Z) + U} \ln(U). \quad (1)$$

The parameters  $A_n(Z)$  and  $B_n(Z)$  are obtained by fitting the calculated DWBA results obtained from the DWION code [14]. Although Eq.(1) represents a convenient approach to generate absolute cross section for the elements and energy range considered, it produces useful results for the overvoltage  $U \leq 10$ . Unfortunately, it does not provide satisfactory results at high and ultra-relativistic energies. As mentioned earlier, the present work proposes a relativistic extension by including in it the Gryzniski type [7], but not exactly similar, relativistic factor  $R(U)$  as given by

$$R(U) = \left( \frac{1+2J}{U+2J} \right) \left( \frac{U+J}{1+J} \right)^{2.02} \times \left[ \frac{(1+U)(U+2J)(1+J)^2}{J^2(1+2J) + U(U+2J)(1+J)^2} \right]^{1.5} \times (1.0 - 0.22U^{0.27} / J^2). \quad (2)$$

The electron approaching the inner-shell electrons feels the atom as an ion of charge  $q = Z - n$ . Here  $Z$  is the atomic number of the atom,  $n$  is the number of electrons up to the shell considered for the ionization and  $J = mc^2 / I$ , where  $m$  is the mass of the electron and  $c$  is the speed of light in vacuum. There are evidences that there is ionic enhancement of cross sections. This effect decreases with the increase of energy of the incident electron. Based on this observation, this work proposes an empirical ionic factor with charge  $q$  and energy dependence. The factor is

$$F_{ion}(U) = (1 + \xi \left( \frac{q}{U} \right)^\eta), \quad (3)$$

Here the parameters  $\zeta$  and  $\eta$  are fitted for each contributing shell and subshell. The parameter  $B_n(Z)$  in Eq.(1) is dropped out and the parameter  $A_n(Z)$  is re-defined as

$$A_n(Z) = C_s Z^\lambda. \quad (4)$$

Here the parameters  $C_s$  and  $\lambda$  are fitted for each contributing shell. The new model SAKLM model proposed is

$$\sigma_{new}(U) = R(U)F_{ion}(U)A_n(Z)N \frac{1}{U} \ln(U). \quad (5)$$

Here  $N$  is the number of electrons in each subshell contributing to total ionization.

### 3. Result and discussion

The ionization potentials  $I$  have been collected from the published results of Desclaux [15]. ISI cross sections are calculated applying the proposed SAKLM model of H, He, C, N, O, Ne, Na, Mg, Si, Cl, Ar, K, Ca, Ti, V, Cr, Co, Ni, Fe, Cu, Zn, Ga, Ge, Se, Sr, Kr, Rb, Y, Mo, Pd, Ag, In, Sn, Xe, Ho, Ta, Au, Pb, Bi, and U for  $K$ -shell, Ar, Ba, Ag, Ho, Ta, Au, Pb, Pd, Sn, Y, U for  $L$ -shell, Pb, Bi, and U for  $M$ -shell, and Au, Pb and Bi for  $L$ -subshell respectively, for the incident electron energies from threshold to 2 GeV for  $K$ -shell and up to 900 MeV for  $L$ -shell,  $L$ -subshell and  $M$ -shell. The calculated results are presented and discussed only for He, C, Ne, Si, Ar, Ni, Mo, Ag, Sn, Au, Bi, and U for  $K$ -shell, Ag, Ba, Ho, Ta, Au, Pb, and U for  $L$ -shell, and Pb, Bi, and U for  $M$ -shell, and Au, Pb and Bi for  $L$ -subshell respectively, for the sake of space. Most recent experimental as well as theoretical results are taken into consideration for comparison with the results obtained by the SAKLM model.

The parameter values  $\zeta$  and  $\eta$  for the ionic factor  $F_{ion}$  in Eq. (3), and  $C_s$  and  $\lambda$  in Eq. (4) are optimized to get the fit for available experimental data over incident energies and for the targets considered herein and presented in table 1. The measure of the quality of best fit is determined by minimizing the chi-square defined as

$$\chi^2 = \sum_i \left[ \frac{\sigma_{cal}(E_i) - \sigma_{exp}(E_i)}{\sigma_{exp}(E_i)} \right]^2,$$

where  $\sigma_{cal}(E_i)$  and  $\sigma_{exp}(E_i)$  refer, respectively, to the calculated and experimental cross sections at the energy point  $E_i$ . The optimum values of the parameters  $\zeta$ ,  $\eta$ ,  $C_s$  and  $\lambda$  are obtained using a non-linear least-square fitting program for the  $K$ -,  $L$ -,  $M$ -shells and  $L$ -subshell ionization. The values of  $A_n$  are plotted in figure 1 as a function of  $Z$ . It is observed, from the figure, that  $A_n(Z)$  exhibits a monotonic decrease with  $Z$  for  $K$ -,  $L$ -,  $M$ -shells and  $L$ -subshell. The smooth trends of

$A_n(Z)$  dictate us that  $A_n(Z)$  can easily be expressed as a function of  $Z$ . The resulting expressions that represent the behavior of  $A_n(Z)$  for the respective shells and subshell are presented in Table 1.

A detailed comparison, for example, for the  $L$ -shell ISI cross sections of the SAKLM and Campos et al (here after will be called CVTS model) models along with the experimental Palinkas et al [16], Middleman et al [17], Hoffmann et al [18], Ishii et al [19], relativistic plane wave Born approximation (RPWBA) of Scofield [20], plane wave Born approximation (PWBA) of Khare et al [21] and empirical GKLW [22] calculations are sketched in figure 2 for Au, respectively. It is evident from the figure that the CVTS model fails, though Campos et al did not claim, to describe cross sections for the overvoltage greater than 10. GKLW and SAKLM models calculate little bit higher cross sections in the peak and in the high- energy regimes, respectively. However, the overall performance of the SAKLM and GKLW models are comparable and calculate cross sections within the experimental error.

The ISI cross sections for  $K$ -shell of He, C, Ne, Si, Ar, and Ni are shown in the figures 3(a)-3(f), respectively. The data are collected from [23-27] for He, [13,19,21,23,28,29] for C, [22,27,28,30,31] for Ne, [13,18,19,23,27,30,32] for Si, [14,18,20,23,30,33,34] for Ar, [13,18,20,23,27,35-38] for Ni, respectively. The MRDM model [27] describes fairly well cross sections in the low energy region but little bit underestimates in the high-energy region, especially for Si and Ne. The SAKLM predictions agree well with the experimental and MRDM results over the wide range of incident energies from threshold to  $10^9$  eV except He in the low energy region. As mentioned earlier that CVTS calculations underestimate the experimental findings in the high-energy region. Not only that the SAKLM provides better agreement than those of the analytical models considered herein for comparison. In the figure 3(e) and 3(f) show good agreement between SAKLM cross section and the quantum mechanical cross sections of Schofield [20] and Khare et al [21] over the entire energy region.

Figures 4(a-f) also show the  $K$ -shell ionization cross-sections of Mo, Ag, Sn, Au, Bi, and U, respectively. The experimental and calculated data are collected from [17,19,22,26,38-41] for Mo, [14,18,20,23,27,36,42-46] for Ag, [18,19,21,23,27,36,44,46] for Sn, [13,17,18,20,23,27,36,37,45-47] for Au, [17-20,23,27,36] for Bi, and [19,20,23,27] for U, respectively. MBELL and MRDM models underestimate the quantum calculations as well as experimental results at high incident energies for U as can be observed from the figures, but SAKLM model provides the better performance among other models for all targets except Sn in the high energy regime. Also it is evident from the Figs. 4(b)-4(f) that the agreement between SAKLM model, and the quantum mechanical RPWBA and PWBA calculations is good for all the targets.

Electron impact  $L$ -shell ionization cross sections for Ag, Ba, Ho, Ta, Pb, and U are presented in figures 5(a)-5(f), respectively. The experimental and calculated data are collected from [18-22] for Ag, [19,20,23] for Ba and Ho, [17,18,21- 22,48] for Ta, [16,18,19,21-22] for Pb, and [18-22] for U, respectively. As seen from the figures that SAKLM model produces better agreement with the experimental results compared with the quantum mechanical RPWBA, PWBA and empirical calculations.

Figures 6(a)-6(c) show the electron impact  $M$ -shell ionization cross sections for Pb, Bi, and U, respectively. The experimental and calculated data are collected from [18,19,21-23] for Pb and Bi, and [18,21-23] for U, respectively. Discrepancies are observed between the PWBA calculations of Khare et al and experimental results in the overall energy regimes considered. These discrepancies in the low energy region become prominent compared with the high-energy region. As observed from the figures that the SAKLM model provides similar results in the high-energy region where as in the low energy region provides lower cross sections than other models.

Figures 7-9 shows the electron impact  $L1$ -,  $L2$ -, and  $L3$ -subshell ionization cross sections for Au, Pb and Bi, respectively. The experimental and calculated data are collected from Palinkas et al [16] for Au, Pb and Bi of all the three  $L$ -subshell, Shima et al [49] for  $L3$ -subshell of Au, Davis et al [45] for  $L3$ -subshell of Au, RPWBA of Scofield [20] for Au and Bi of all  $L$ -subshell, and PWBA of Khare et al [21] for Au, Pb and Bi of all  $L$ -subshell, respectively. The Figs.7-9 show good agreement between the SAKLM model cross sections and experimental data over the whole energy range. The RPWBA cross section of Scofield [20] are also in good agreement with our present cross sections over the entire energy region for all inner subshells. Good agreement between SAKLM  $L$ -subshell cross-sections and the PWBA cross-sections of Khare et al [21] except  $L2$ -subshell ionization at higher incident energies.

From the above discussions, we notice that the simplified SAKLM model provides better agreements with the experimental results over the entire energy regimes. The important features of the proposed model are that it provides acceptable cross sections with less fitting parameters compared with other models considered.

#### 4. Conclusions

The SAKLM model, from the overall level of its performance, shows better success for the description of the experimental electron impact  $K$ -,  $L$ -,  $M$ - shells, and  $L$ -subshell ionization cross section data for the targets considered with the incident electron energies from threshold to 2 GeV for  $K$ -shell, up to 900 MeV for  $L$ - and  $M$ -shell and up to 600 keV for  $L$ -subshell, respectively. The recent MBELL results are applied to selected targets. However, as compared to other theoretical

results considered herein for comparison, the level of performance of the SAKLM model with respect to the domain of species and incident energies, found the best or better than other complicated quantum, classical, or empirical methods. It is demonstrated that the SAKLM model provides encouraging and reasonably accurate results. The SAKLM model with its simple structure turns out to be a lucrative alternative for the description of electron impact single ionization cross sections for the  $K$ -,  $L$ -,  $M$ -shells, and  $L$ -subshell and may be used conveniently for the fast generation of reasonably accurate cross sections as the practitioners in the applied fields need.

### Acknowledgments

This work was done within the framework of the Associateship Scheme of the Abdus Salam International Centre for Theoretical Physics, Trieste, Italy.

### References

1. C.J. Powell, *Electron Impact Ionization* edited by T.D. Märk and D.H. Dunn (Springer-Verlag, Berlin, 1985).
2. C.J. Powell, *Microbeam Analysis* edited by J.R. Michael and P. Ingram (San Francisco, CA, Francisco Press, 1990).
3. H. Bethe Ann. Phys. **5**, 325 (1930).
4. H. Bethe Phys. **76**, 293 (1930).
5. R. Mayol and F. J. Salvat Phys. B: At. Mol. Opt. Phys. **23**, 2117 (1990).
6. R. Hippler, Phys. Lett. A **144**, 81 (1990).
7. M. Gryzniski, Phys. Rev. A **138**, 305 (1965).
8. Y. –K. Kim, J.P. Santos and F. Parente, Phys. Rev. A **62**, 05210 (2001).
9. H. Deutsch, Margreiter, T.D. Märk, Z Phys. D**29**, 31 (1994).
10. E. Casnati, A. Tartari, C. Baraldi, J. Phys. B: At. Mol. Opt. Phys. **15**, 155 (1982).
11. C. Homberger, J. Phys. B: At. Mol. Opt. Phys. **31**, 3693 (1998).
12. C.H. Tang, An Zhu, X. –Q. Fan, Z. –M. Luo, Chin. Phys. Lett. **18**, 1053 (2001).
13. C.S. Campos, M.A.Z Vasconcellos, J.C. Trincavelli and S. Segui, J. Phys. B: At. Mol. Opt. Phys. **40**, 3835 (2007).
14. S. Segui, M. Dingfelder, F. Salvat, Phys. Rev. A **67**, 062710 (2003).
15. J.P. Desclaux, At. Data Nucl. Data Tables **12**, 325 (1973).
16. J. Palinkas, B. Schlenk, Z. Phys. A **297**, 29 (1980).
17. L.M. Middleman, R.L. Ford and R. Hofstadter. Phys. Rev. A **2**, 1429 (1970).

18. D.H.H. Hoffmann, C. Brendel, H. Genz, W. Low, S. Muller and A. Richter, *Z. Phys. A* **293**, 187 (1979). D.H.H. Hoffmann, H. Genz, W. Low and A. Richter, *Phys. Lett. A* **65**, 304 (1978).
19. K. Ishii, M. Kamiya, K. Sera, S. Morita, H. Tawara, M. Oyamada and T.C. Chu, *Phys. Rev. A* **15**, 906 (1977).
20. J.H. Scofield, *Phys. Rev. A* **18**, 963 (1978).
21. S.P. Khare and J.M. Wadehra, *Can. J. Phys.* **74**, 376 (1996).
22. A.K.F. Haque, M.A. Uddin, M.A.R. Patoary, A.K. Basak, M.R. Talukder, B.C. Saha, K.R. Karim, F.B. Malik, *Eur. Phys. J. D* **42**, 203 (2007).
23. A.K.F. Haque, M.A. Uddin, A.K. Basak, K.R. Karim, B.C. Saha, *Phys. Rev. A* **73**, 012708 (2006); A.K.F. Haque, M.A. Uddin, A.K. Basak, K.R. Karim, B.C. Saha, F.B. Malik, *Phys. Scr. A* **74**, 377 (2006).
24. R. Rejoub, B.G. Lindsay, and R.F. Stebbings, *Phys. Rev. A* **65**, 042713 (2002).
25. P. Nagy, A. Skutlartz and V. Schmidt, *J. Phys. B* **13**, 1249 (1980).
26. M.B. Shah, D.S. Elliott and H.B. Gilbody, *J. Phys. B* **20**, 3501 (1987). M.B. Shah, D.S. Elliott, P. MaCallion and H.B. Gilbody, *J. Phys. B* **21**, 2751 (1988).
27. A.K.F. Haque, M.S.I. Sarker, M.A.R. Patoary, M. Shahjahan, M. Ismail Hossain, M. Alfaz Uddin, A.K. Basak, B.C. Saha, *I. J. Quantum Chem.*, **109**, 1442 (2009).
28. H. Tawara, K.G. Harrison and F.J. De Heer, *Physica* **63**, 351 (1973).
29. R.F. Egerton, *Phil. Mag.* **31**, 199 (1975).
30. H. Platten, G. Schiwietz and G. Nolte, *Phys. Lett. A* **107**, 83 (1985).
31. G. Glupe and W. Mehlhorn, *J. Physique, Suppl.* 32 (1971) C4-40. G. Glupe and W. Mehlhorn, *Phys. Lett. A* **25**, 274 (1967).
32. A.V. Shchagin, V. I. Pristupa, N.A. Khizhnyak, *Nucl. Instrum. Methods Phys. Res. B* **84**, 9 (1994).
33. C.A. Quarles, *Phys. Rev. A* **13**, 1278 (1975). C. Quarles and M. Semaan, *Phys. Rev. A* **26**, 3147 (1982).
34. R. Hippler, K. Saeed, I. McGregor and H. Kleinpoppen, *Z. Phys. A* **307**, 83 (1982).
35. A.E. Smick and P. Kirkpatrick, *Phys. Rev.* **67**, 153 (1945).
36. W. Scholz, A. Li-Scholz, R. Colle and I.L. Preiss, *Phys. Rev. Lett.* **29** (1972) 761. A. Li-Scholz, R. Colle, I.L. Preiss and W. Scholz, *Phys. Rev. A* **7**, 1957 (1973).
37. J. Jessenberger and W. Hink, *Z. Phys. A* **275**, 331 (1975).
38. H. Genz, C. Brendel, P. Eschwey, U. Kuhn, W. Low, A. Richter and P. Seserko, *Z. Phys.* **305**, 9 (1982).

39. F.Q. He, X.G. Long, Z.F. Peng, Z.M. Luo and Z. An, Nucl. Instrum. Methods B **114** 213 (1996).  
Z.M. Luo, Z. An, T.H. Li, L.M. Wang, Q. Zhu, and X.Y. Xia, J. Phys. B **30**, 2681 (1997). F.Q. He, X.G. Long, X.F. Peng, Z.M. Luo and Z. An, Acta Physica Sinica **5**, 449 (1996). F.Q. He, Z.F. Peng, X.G. Long, Z.M. Luo and Z. An, Nucl. Instrum. Methods B **129**, 445 (1997).
40. Z.M. Luo, Z. An, F.Q. He, T. H. Li, X.G. Long and X.F. Peng, J. Phys. B **29** (1996) 4001. Z.M. Luo, Z. An, T.H. Li, L.M. Wang, Q. Zhu, and X.Y. Xia, J. Phys. B **30**, 2681 (1997).
41. S. Luo, D. C. Joy, *Microbeam Analysis*, edited by D. G. Howitt, (San Francisco, CA, Francisco Press, 1991), 67.
42. B. Schlenk, D. Berenyi, S. Riez, A. Valek and G. Hock, Acta Phys. Hung. **41**, 159 (1976).
43. S.A.H. Seif el Naser, D. Berenyi and G. Bibok, Z. Phys. **267**, 169 (1974).
44. S. Riez, B. Schlenk, D. Berenyi, G. Hock and A. Valek, Acta Phys. Hung. **42**, 269 (1977).
45. D.V. Davis, V.D. Mistry and C.A. Quarles, Phys. Lett. **38A**, 169 (1972).
46. D.H Rester and W.E. Dance, Phys. Rev. **152**, 1 (1966).
47. K.H. Berkner, S.N. Kaplan and R.V. Pyle, Bull. Am. Phys. Soc. **15**, 786 (1970).
48. S. Reusch, H. Genz, W. Low, A. Richer, Z. Phys. D **3**, 379 (1986).
49. K. Shima, T. Nakagawa, K. Umetani, and T. Mikumo, Phys. Rev. A **24**, 72(1981).

Table 1. Expressions obtained for the parameter  $A_n$  as the function of atomic number  $Z$  for  $K$ -,  $L$ -,  $M$ -shells, and  $L$ -subshell and the ionic parameters  $\xi$  and  $\eta$ .

Shell/Subshell	$C_s$	$\lambda$	Parameter $A_n$	$\xi$	$\eta$
$K$	11.5	-4.35	$A_n = 11.5 \times Z^{-4.35}$	0.01	1.0
$L$	5500	-4.95	$A_n = 5500 \times Z^{-4.95}$	0.01	1.0
$L1$	3100	-4.90	$A_n = 3100 \times Z^{-4.90}$	0.01	1.1
$L2$	3200	-4.84	$A_n = 3200 \times Z^{-4.84}$	0.01	1.1
$L3$	3250	-4.77	$A_n = 3250 \times Z^{-4.77}$	0.01	1.1
$M$	5700	-4.25	$A_n = 5700 \times Z^{-4.25}$	0.01	1.0

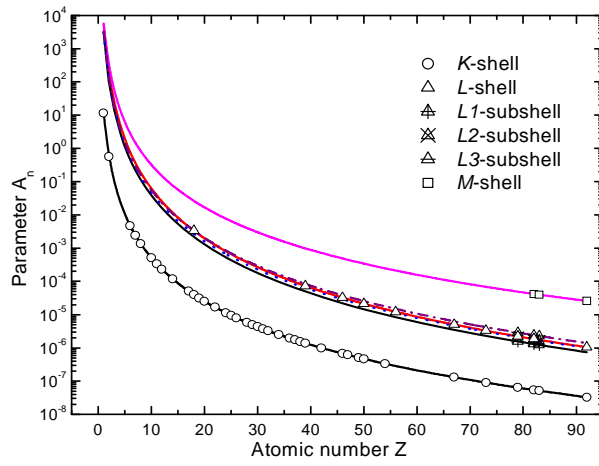


Figure 1. Variation of parameter  $A_n$  with atomic number  $Z$ .

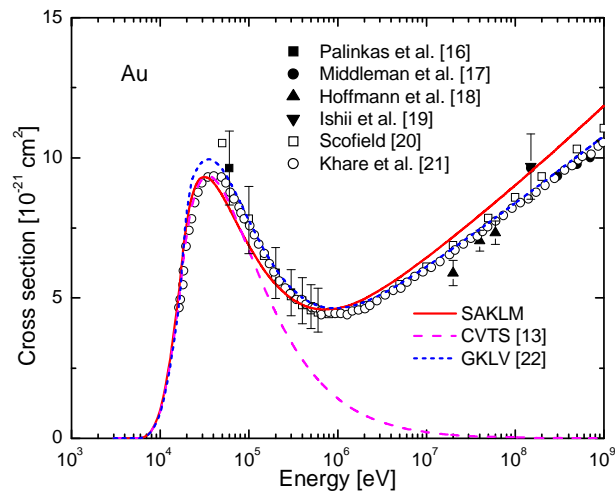


Figure 2. Electron impact  $L$ -shell ionization cross-section of Au.

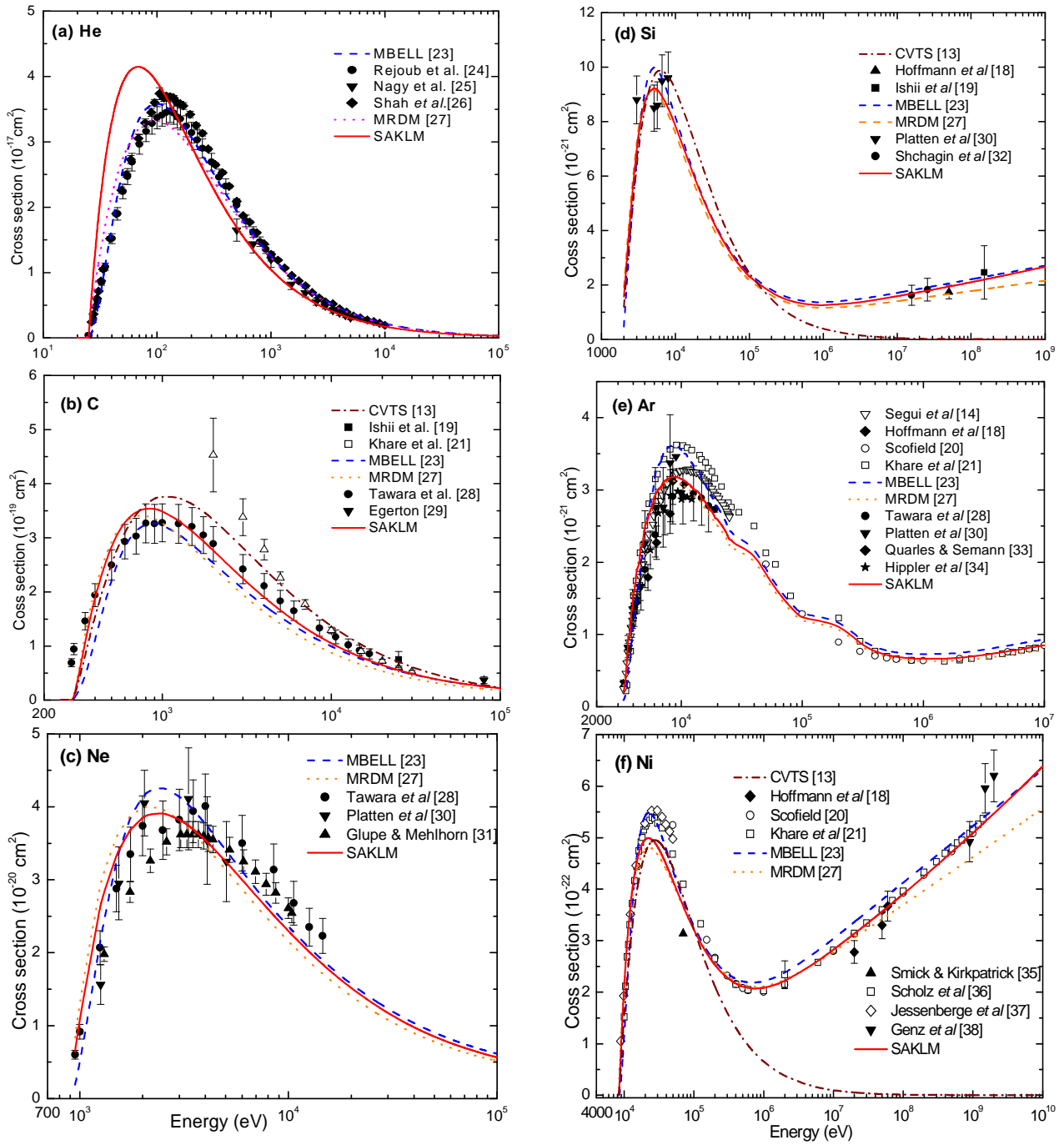


Figure 3. Electron impact ionization cross-sections for K-shell: (a) He, (b) C, (c) Ne, (d) Si, (e) Ar, (f) Ni.

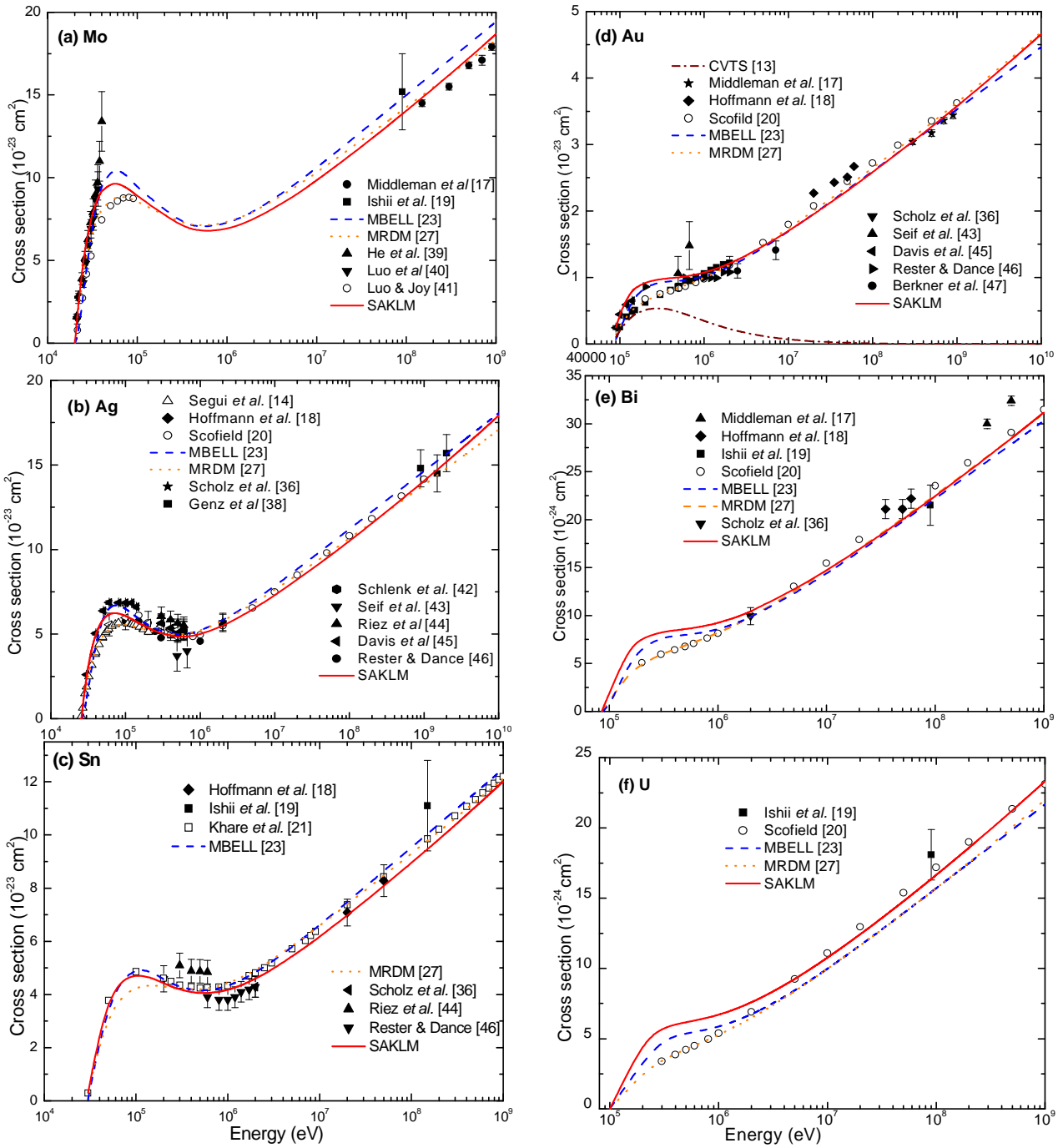


Figure 4. Same as in Figure 3 for: (a) Mo, (b) Ag, (c) Sn, (d) Au, (e) Bi and (f) U.

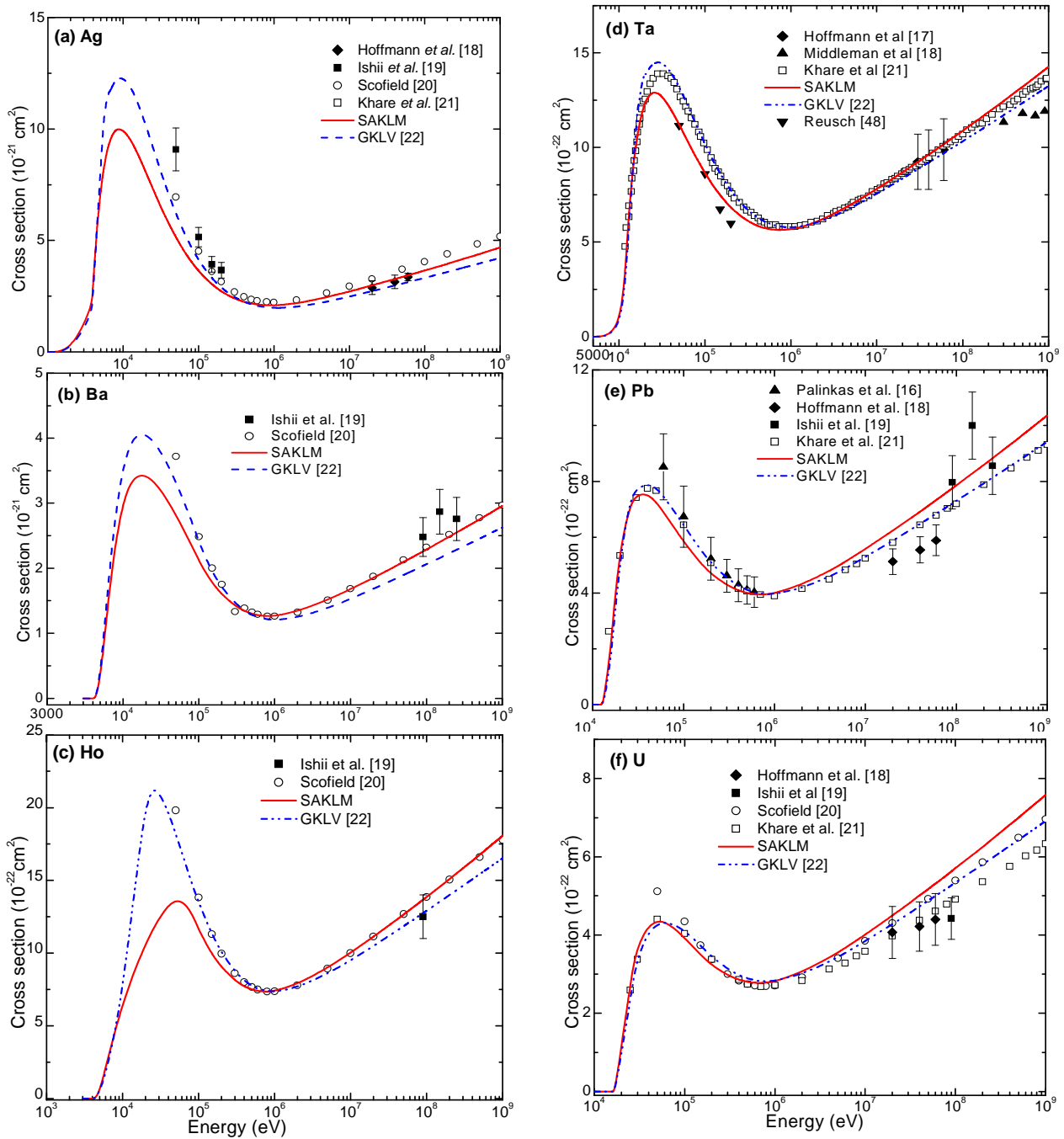


Figure 5. Electron impact ionization cross-sections for *L*-shell: (a) Ag, (b) Ba, (c) Ho, (d) Ta, (e) Pb, (f) U.

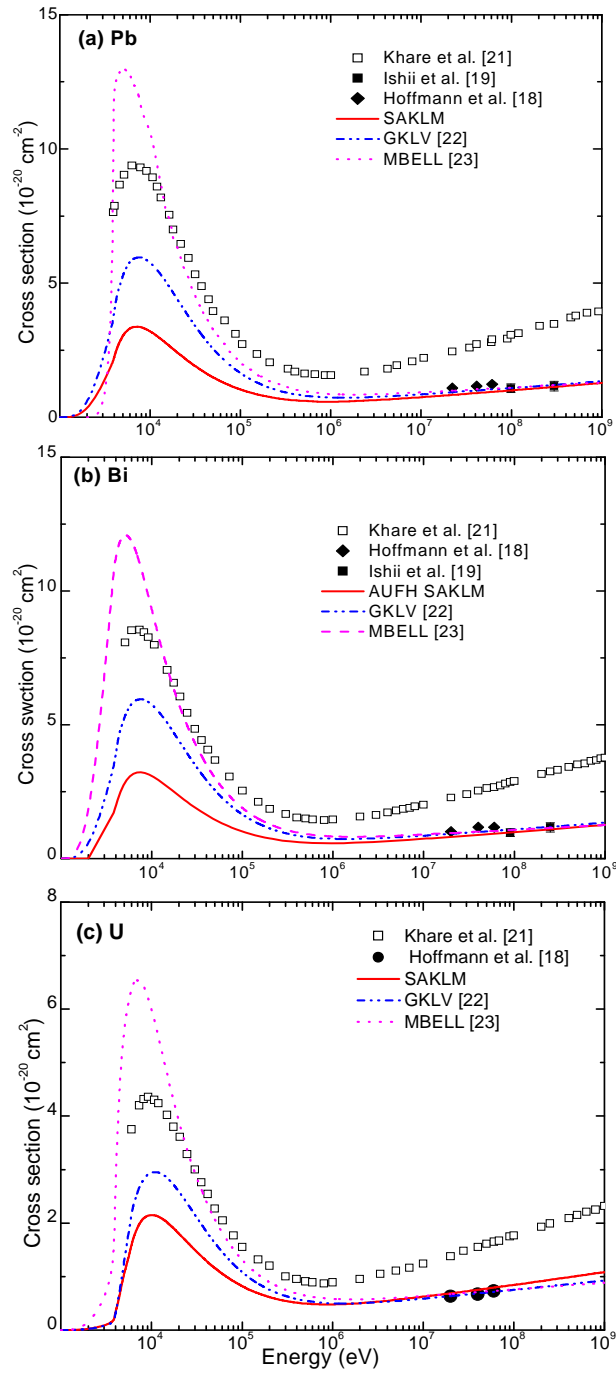


Figure 6. Electron impact ionization cross-sections for *M*-shell: (a) Pb, (b) Bi, (c) U.

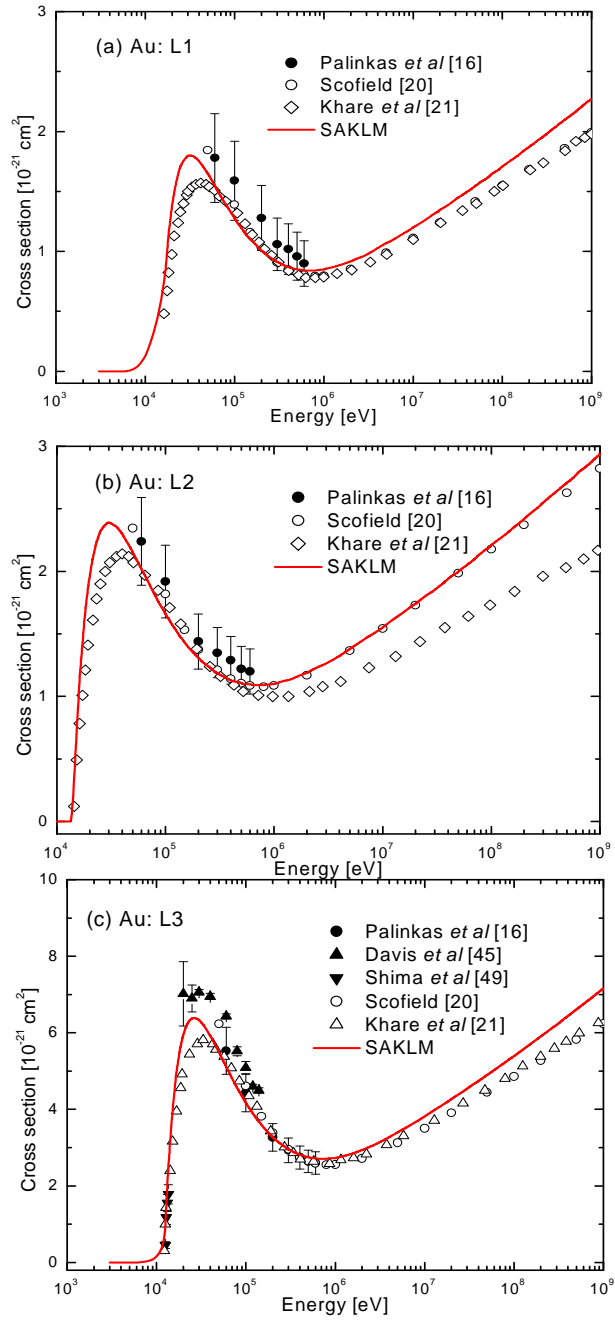


Figure 7. Electron impact  $L$ -subshell ionization cross-sections of Au for: (a)  $L1$ , (b)  $L2$ , and (c)  $L3$ .

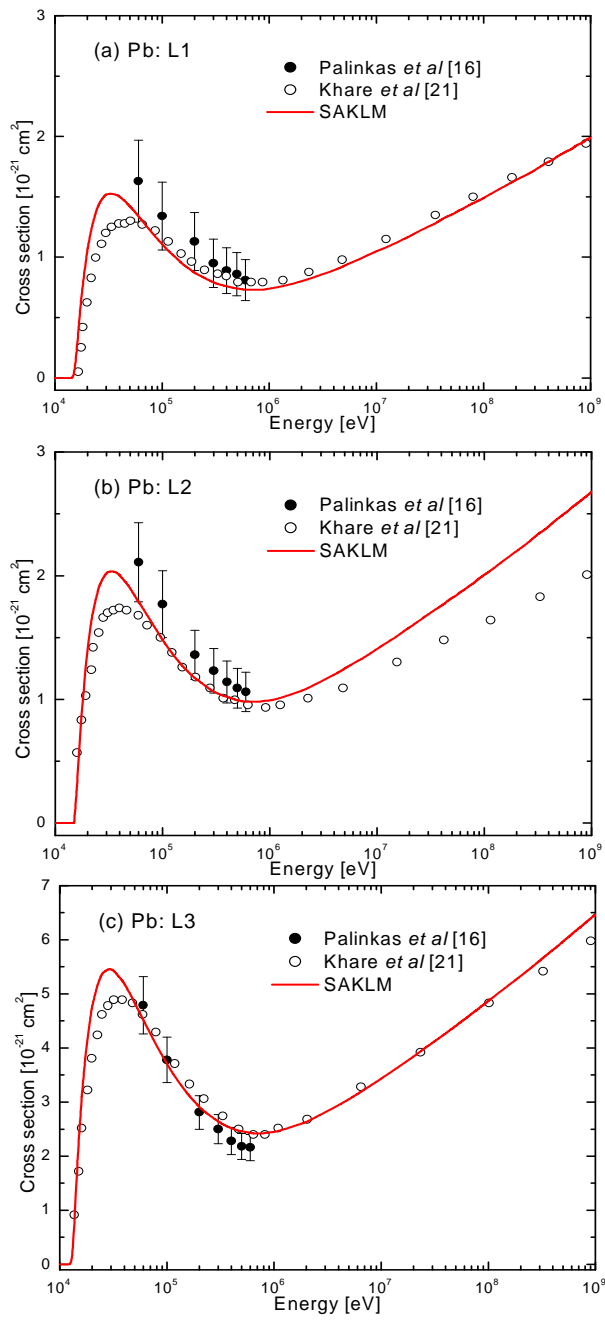


Figure 8. Electron impact  $L$ -subshell ionization cross-sections of Pb for: (a)  $L1$ , (b)  $L2$ , and (c)  $L3$ .

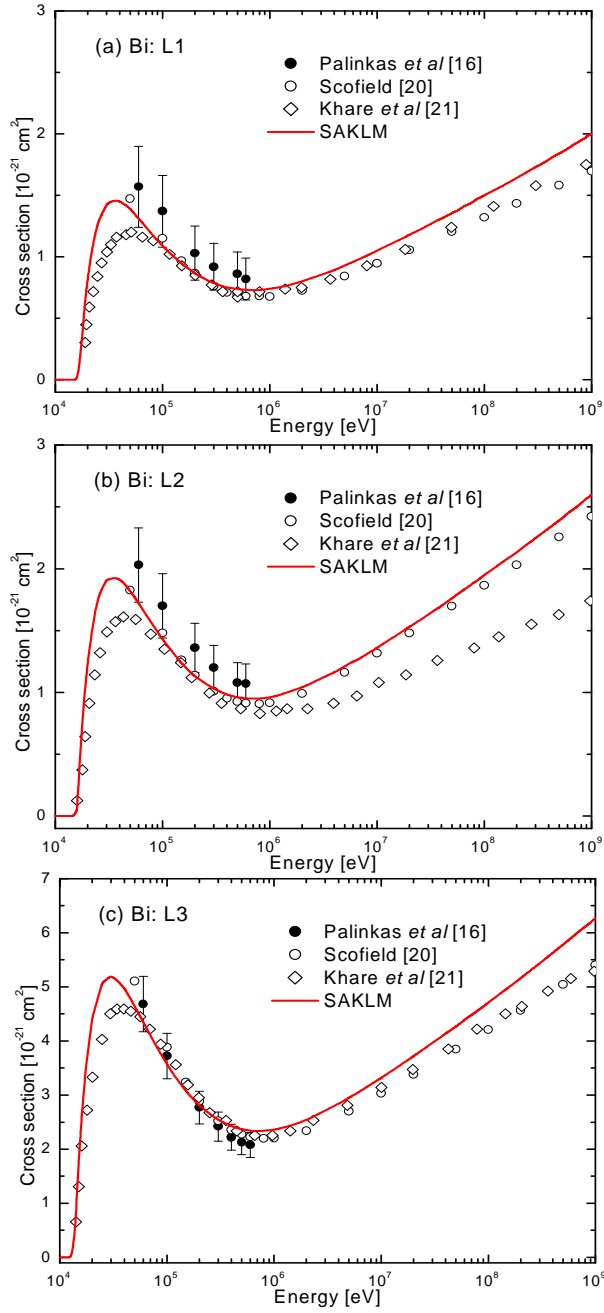


Figure 9. Electron impact  $L$ -subshell ionization cross-sections of Pb for: (a)  $L1$ , (b)  $L2$ , and (c)  $L3$ .